

A glycomics and proteomics study of aging and Parkinson's disease in human brain

Rekha Raghunathan¹, John D. Hogan³, Adam Labadorf³, Richard H. Myers^{1,3,4},
and Joseph Zaia^{1,2,3,*}

¹ Boston University, Molecular and Translational Medicine, Boston, 02118, USA

² Boston University, Biochemistry, Boston, 02118, USA

³ Boston University, Bioinformatics Program, Boston, 02118, USA

⁴ Boston University, Department of Neurology, Boston, 02118, USA

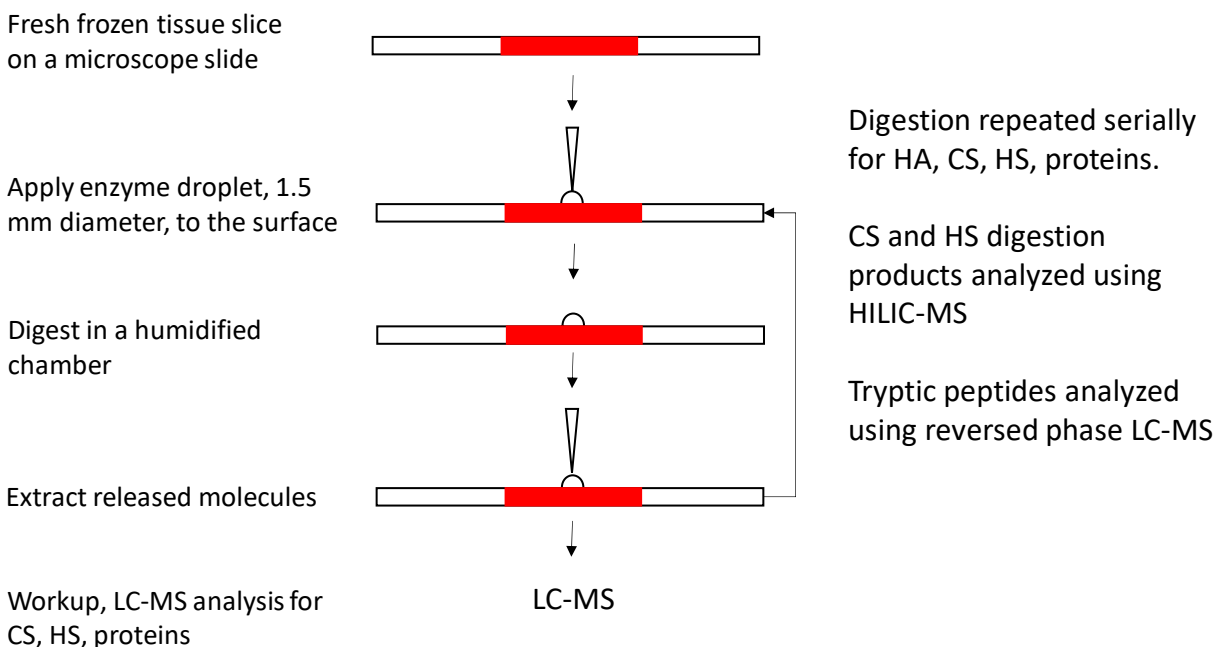
Supplementary Material

Supplementary Figures..... p. 2

Supplementary Tables.....p. 20

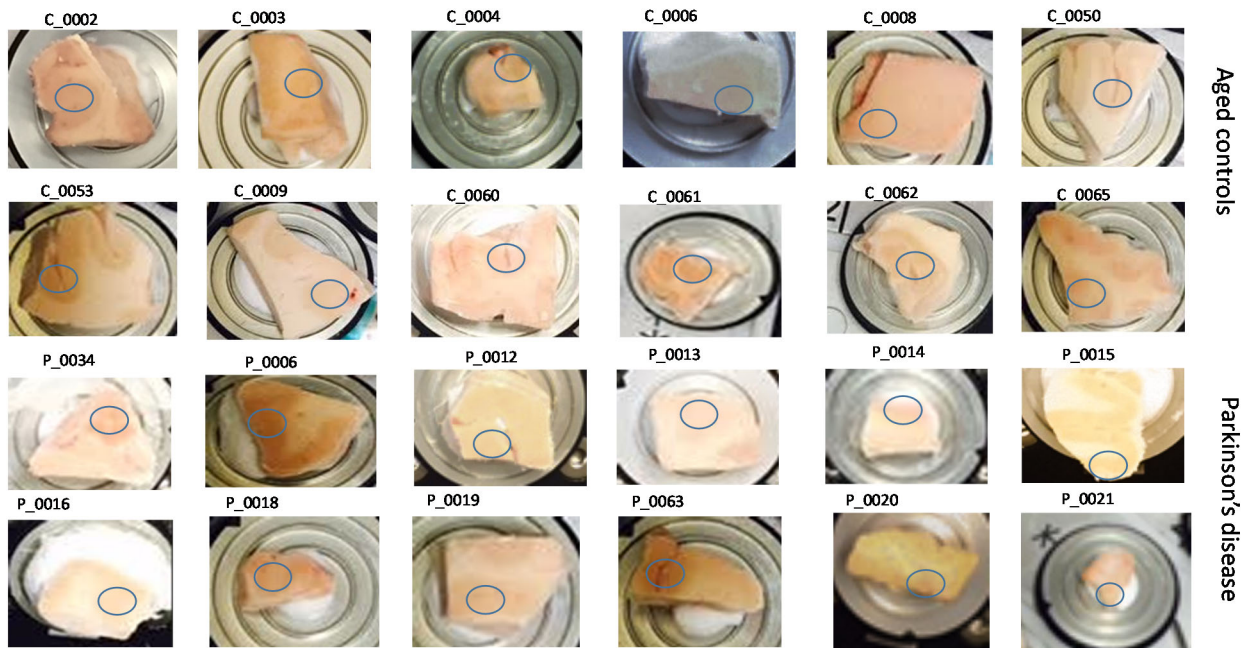
Supplementary References.....p. 30

Supplementary Figure S 1. (A) Tissue omics workflow ¹. Fresh frozen brain tissue was cryosectioned and mounted on microscope slides. A 5 mm diameter droplet of enzyme solution was applied to the tissue surface. The slides were transferred to a humidified chamber and allowed to digest. The digestion products were extracted by pipetting. The digestion products were cleaned and then analyzed using LC-MS. The process was repeated for three glycosidases (hyaluronidase, chondroitinases, heparin lyases) and trypsin. Abbreviations: HA, hyaluronan; CS, chondroitin sulfate; HS, heparan sulfate; LC-MS, liquid chromatography-mass spectrometry; HILIC, hydrophilic interaction chromatography.

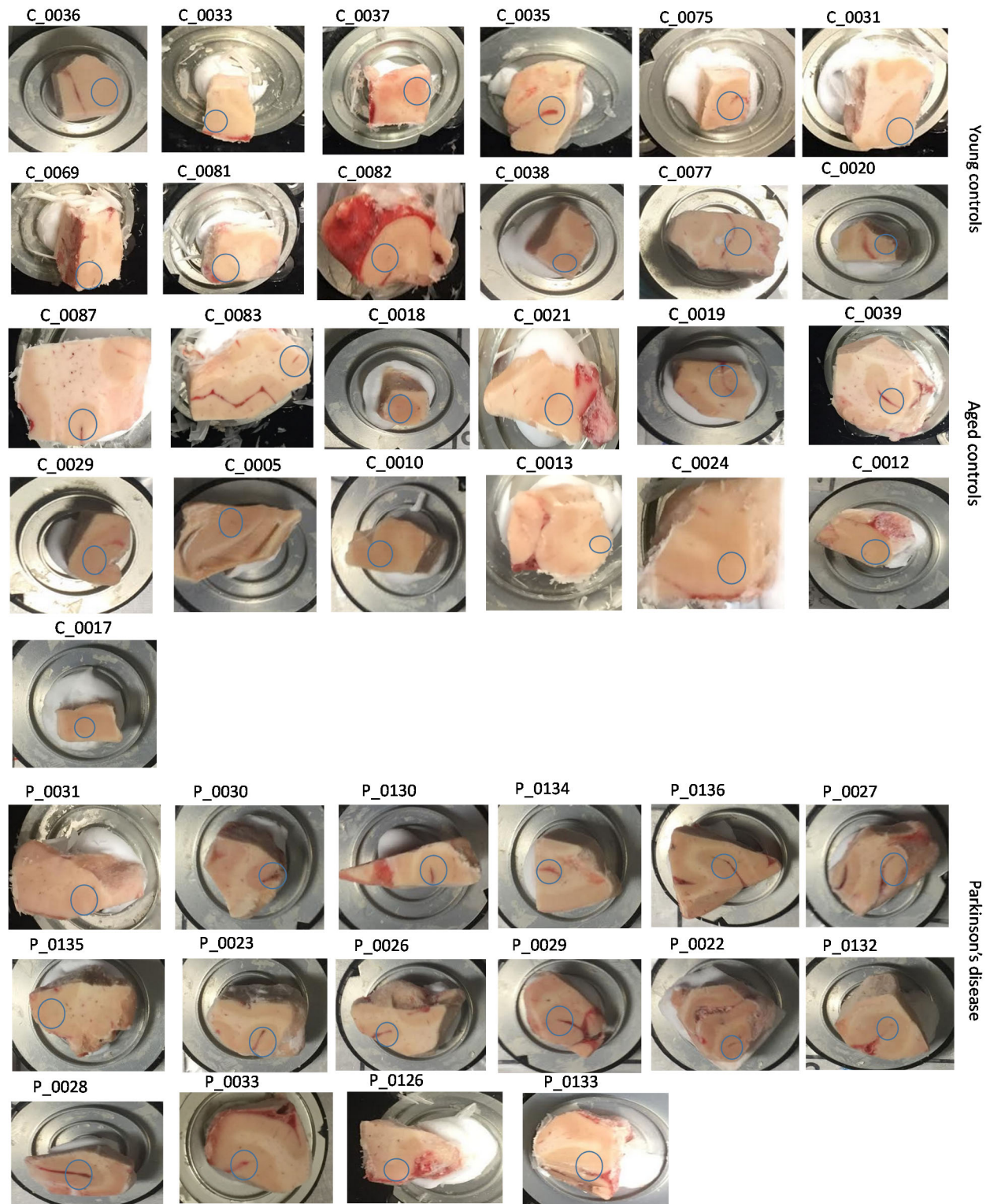


Supplementary Figure S 1B. Photographic images of the brain tissue blocks used in the aging and PD study, mounted on cryotome chucks. The 5 mm diameter grey matter areas to which enzyme digestion solution was applied on tissue slices prepared from these tissue blocks are marked with blue circles.

Cohort 1

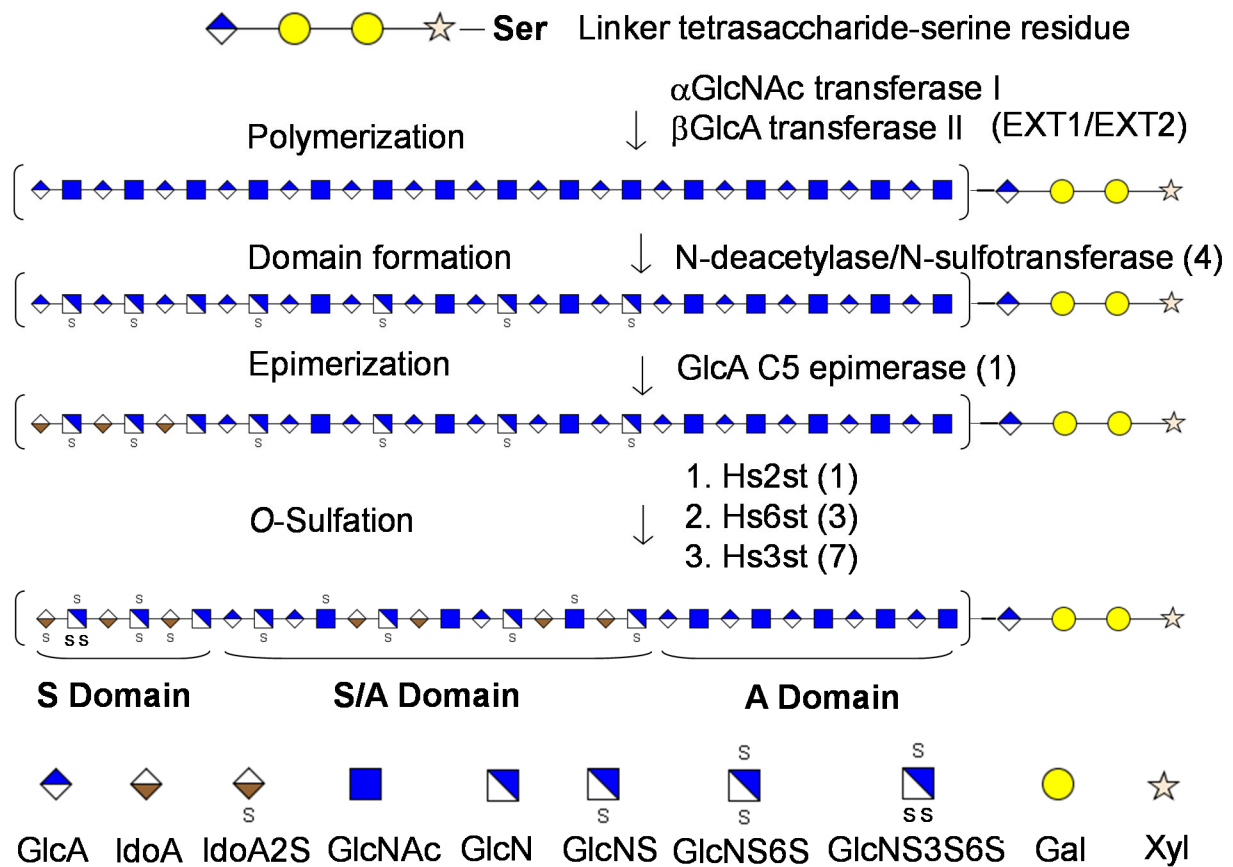


Supplemental Figure 1B (continued) Cohort 2

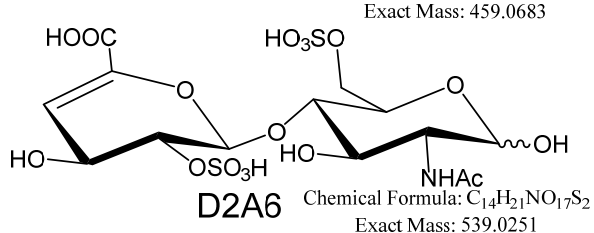
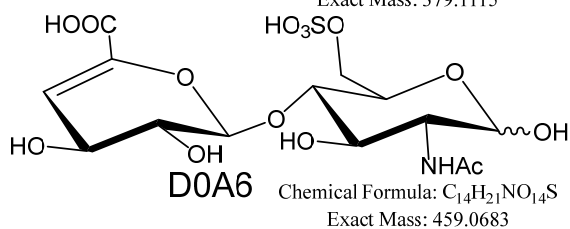
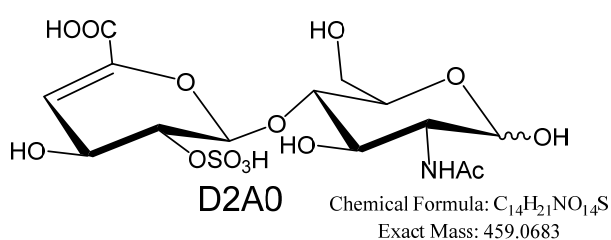
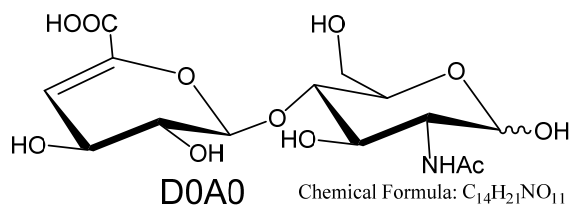
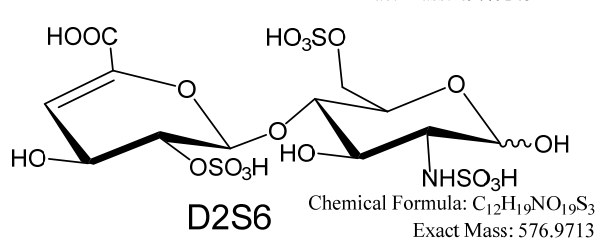
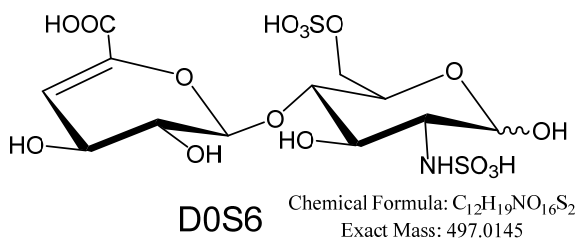
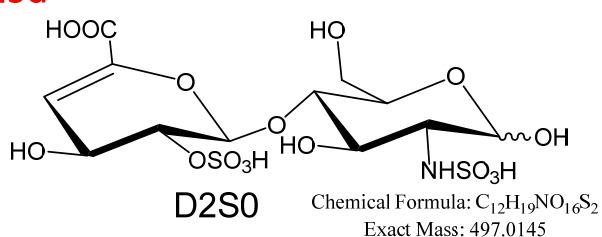
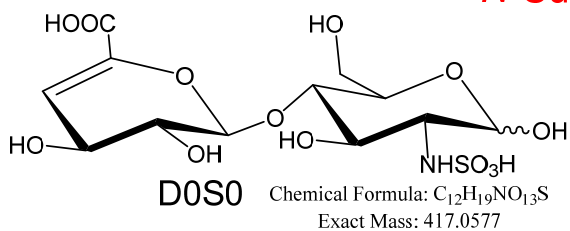


Supplementary Figure S 2. Biosynthesis of heparan sulfate (HS)². Chains are biosynthesized by a series of enzymes in the endoplasmic reticulum and Golgi apparatus. The mature chains have a structure consisting of domains of high, low, and intermediate degree of sulfation. The structures and patterns of these domains varies in a spatially and temporally regulated manner³.

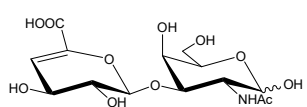
Biosynthesis of heparin and heparan sulfate



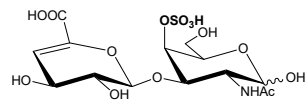
Supplementary Figure S 3. Nomenclature of HS disaccharides

N-Acetylated**N-Sulfated**

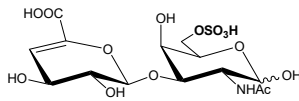
Supplementary Figure S 4. Nomenclature of CS disaccharides

**D0a0**

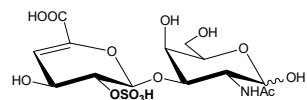
$C_{14}H_{21}NO_{11}$
Exact Mass: 379.11

**D0a4**

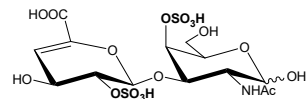
$C_{14}H_{21}NO_{13}S$
Exact Mass: 459.07

**D0a6**

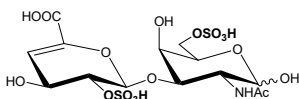
$C_{14}H_{21}NO_{14}S$
Exact Mass: 459.07

**D2a0**

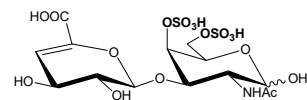
$C_{14}H_{21}NO_{14}S$
Exact Mass: 459.07

**D2a4**

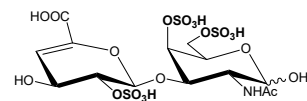
$C_{14}H_{21}NO_{17}S_2$
Exact Mass: 539.03

**D2a6**

$C_{14}H_{21}NO_{17}S_2$
Exact Mass: 539.03

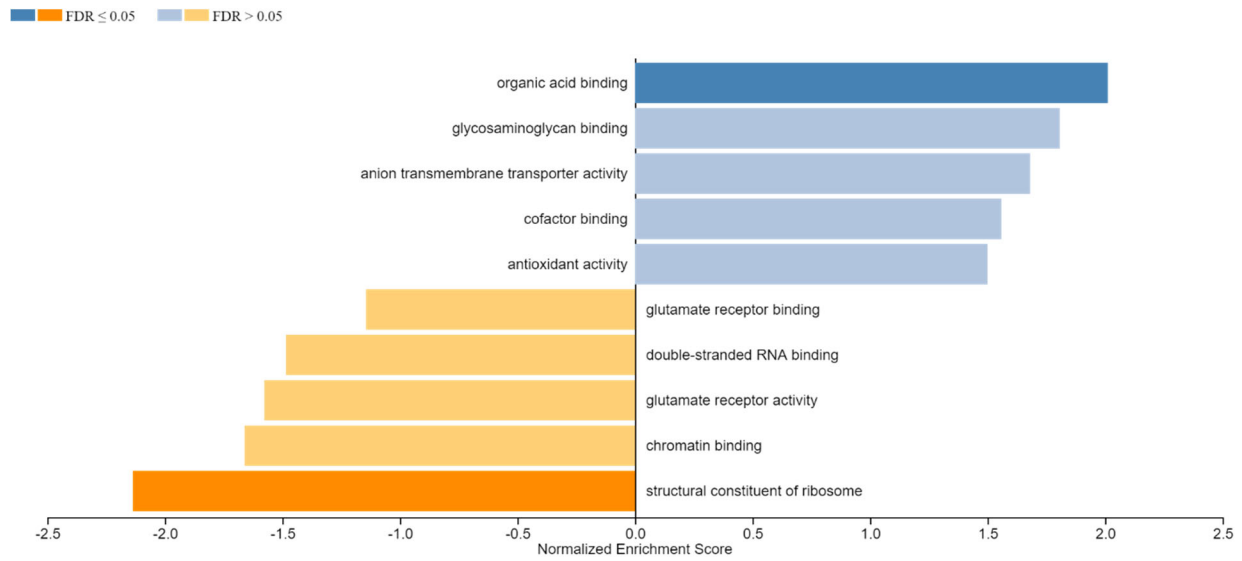
**D0a10**

$C_{14}H_{21}NO_{17}S_2$
Exact Mass: 539.03

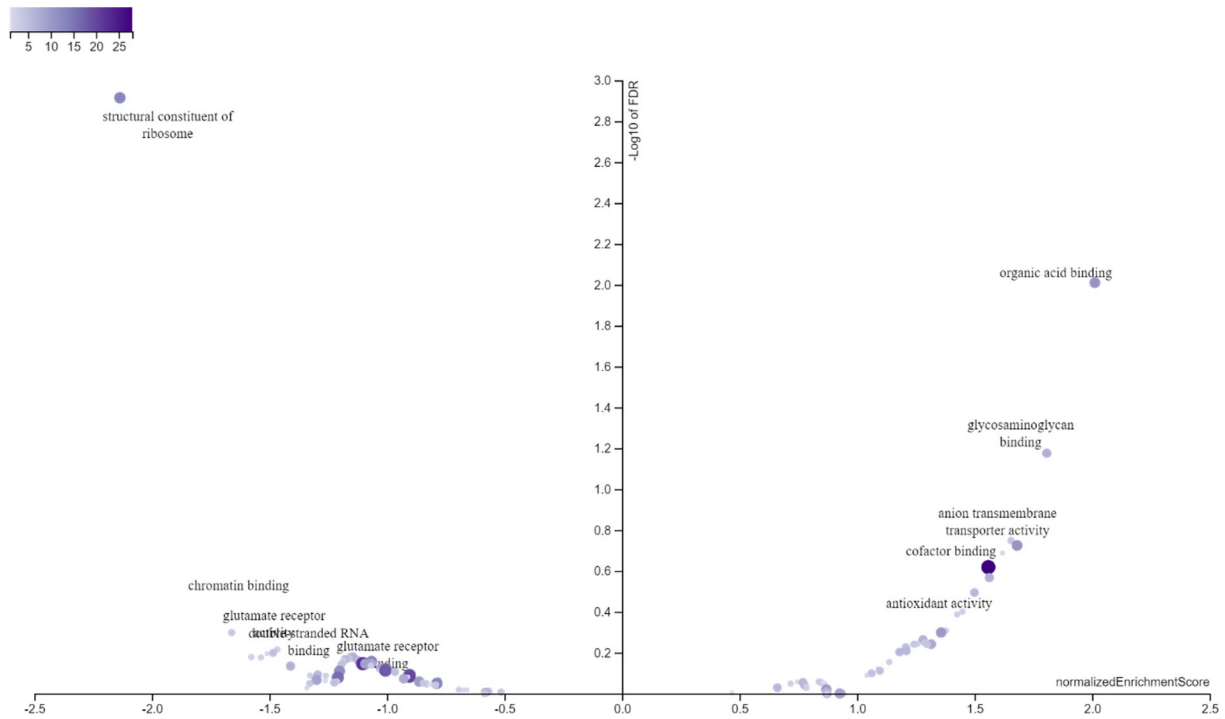
**D2a10**

$C_{14}H_{21}NO_{20}S_3$
Exact Mass: 618.98

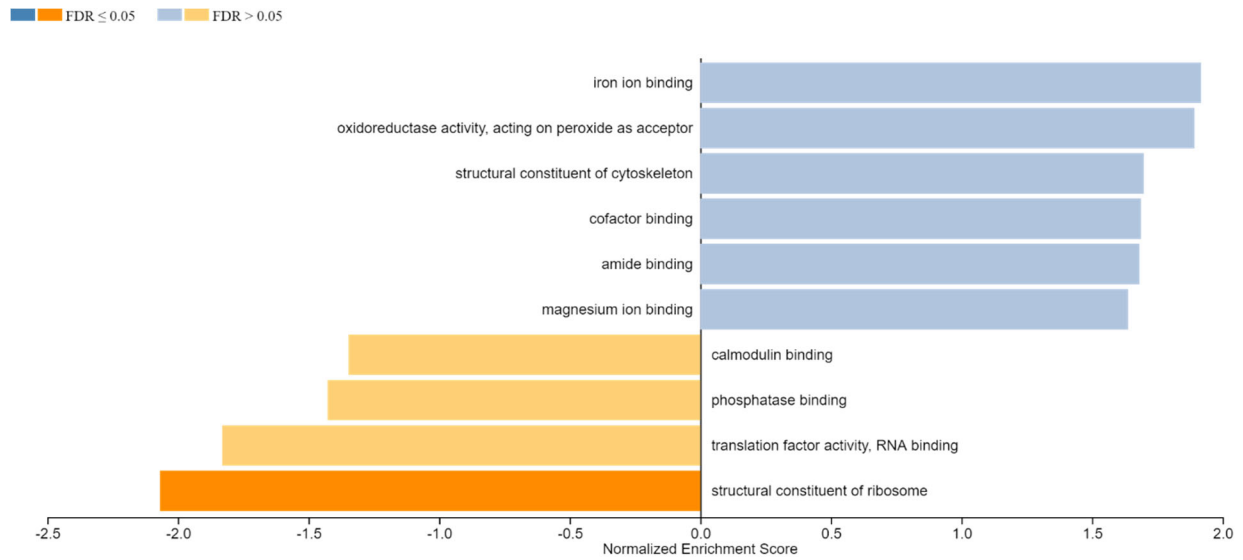
Supplementary Figure S 5. GSEA of differentially expressed proteins young versus aged rat striatum from previously published data⁴. (A) Bar plot showing enriched gene sets.



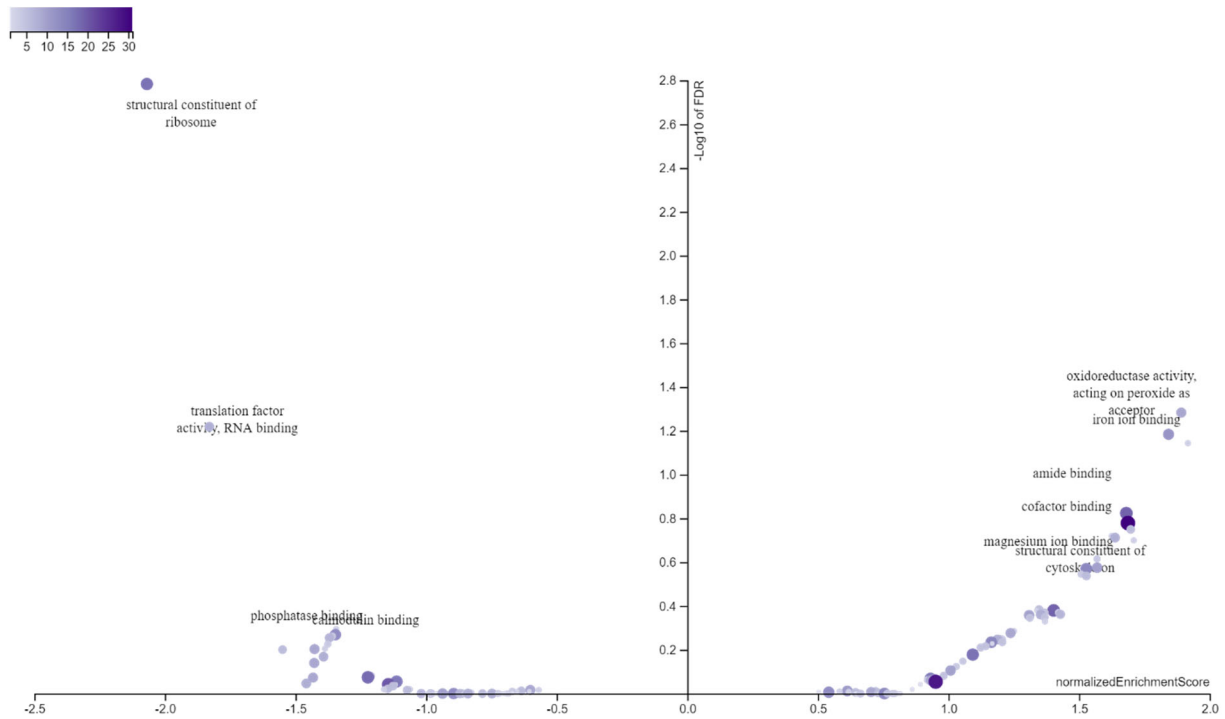
Supplementary Figure S 5. GSEA of differentially expressed proteins young versus aged rat striatum from previously published data⁴. (B) Volcano plot showing most enriched molecular functions.



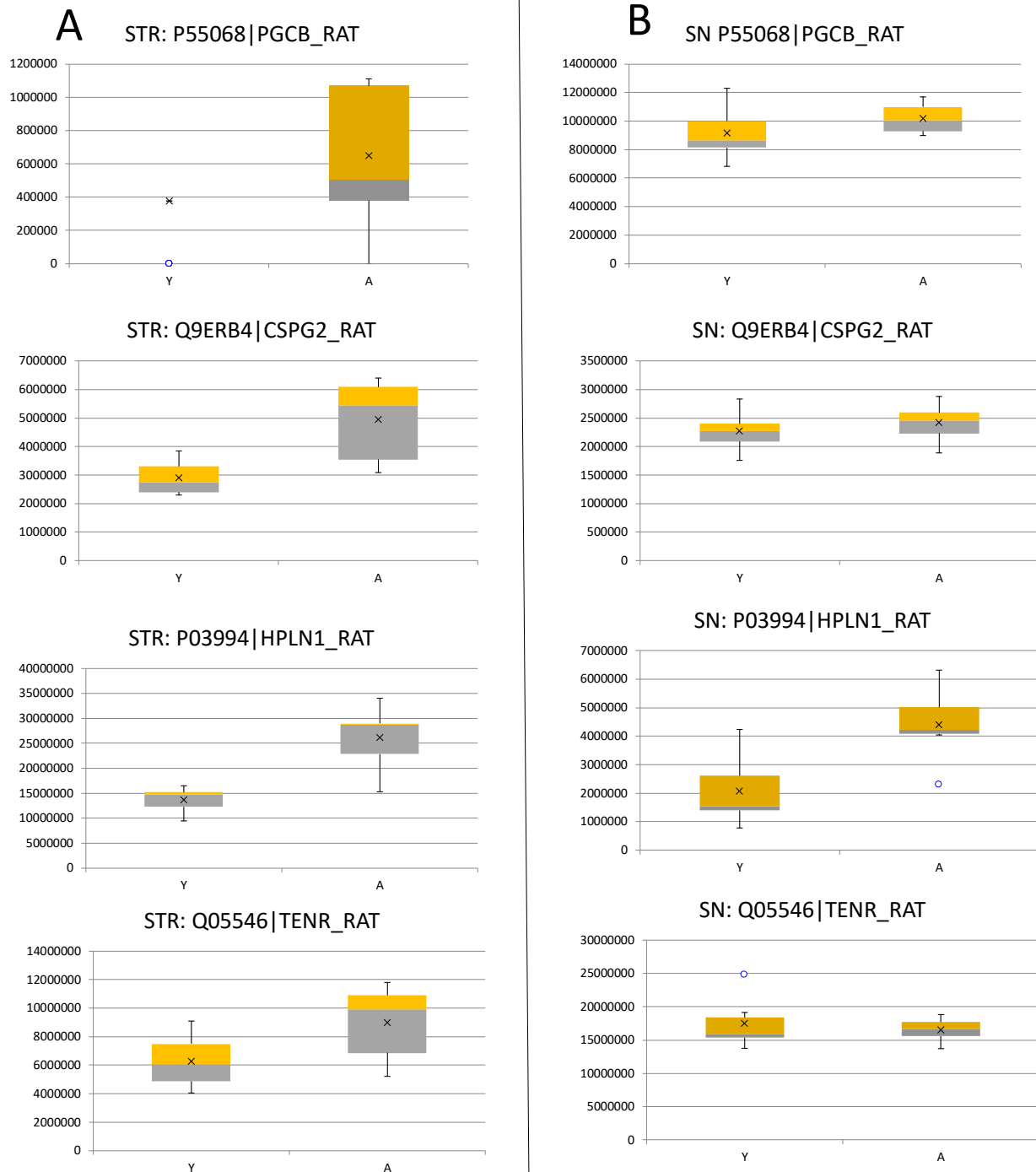
Supplementary Figure S 6. GSEA of differentially expressed proteins in young versus aged rat substantia nigra from previously published data⁴. (A) Bar plot showing enriched gene sets.



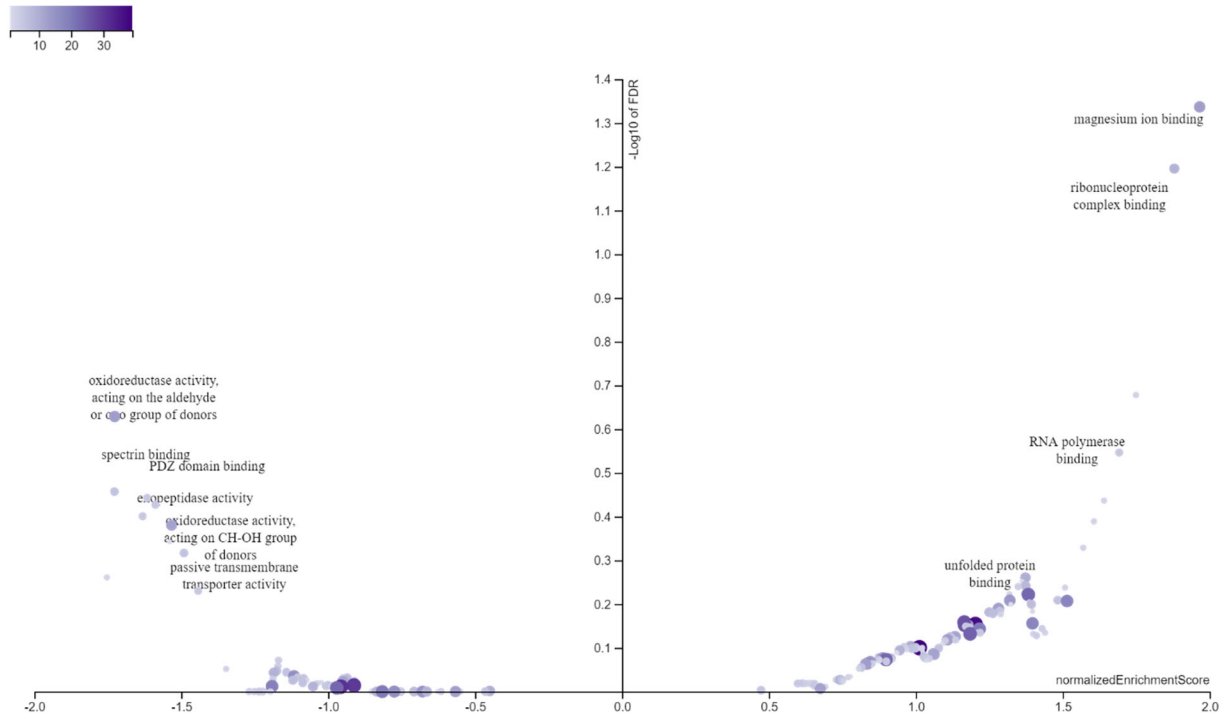
Supplementary Figure S 6. GSEA of differentially expressed proteins in young versus aged rat substantia nigra from previously published data⁴. (B) Volcano plot showing most enriched molecular functions.



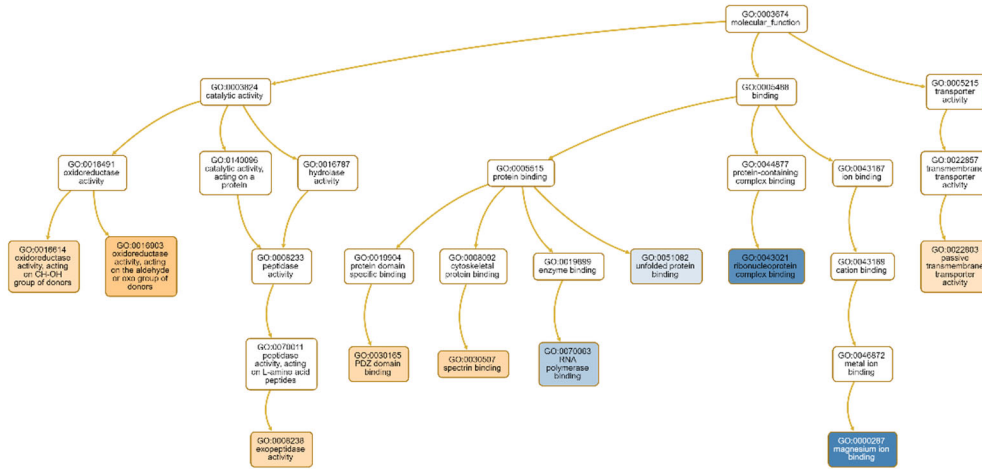
Supplementary Figure S 7. Comparison of PNN-associated protein abundances in young vs aged rat brain (A) striatum (STR) and (B) substantia nigra (SN) from previously published data⁴.



Supplementary Figure S 8. GSEA of differentially expressed human proteins young (<60 years) versus aged (>60 years). (A) Volcano plot showing most enriched molecular functions

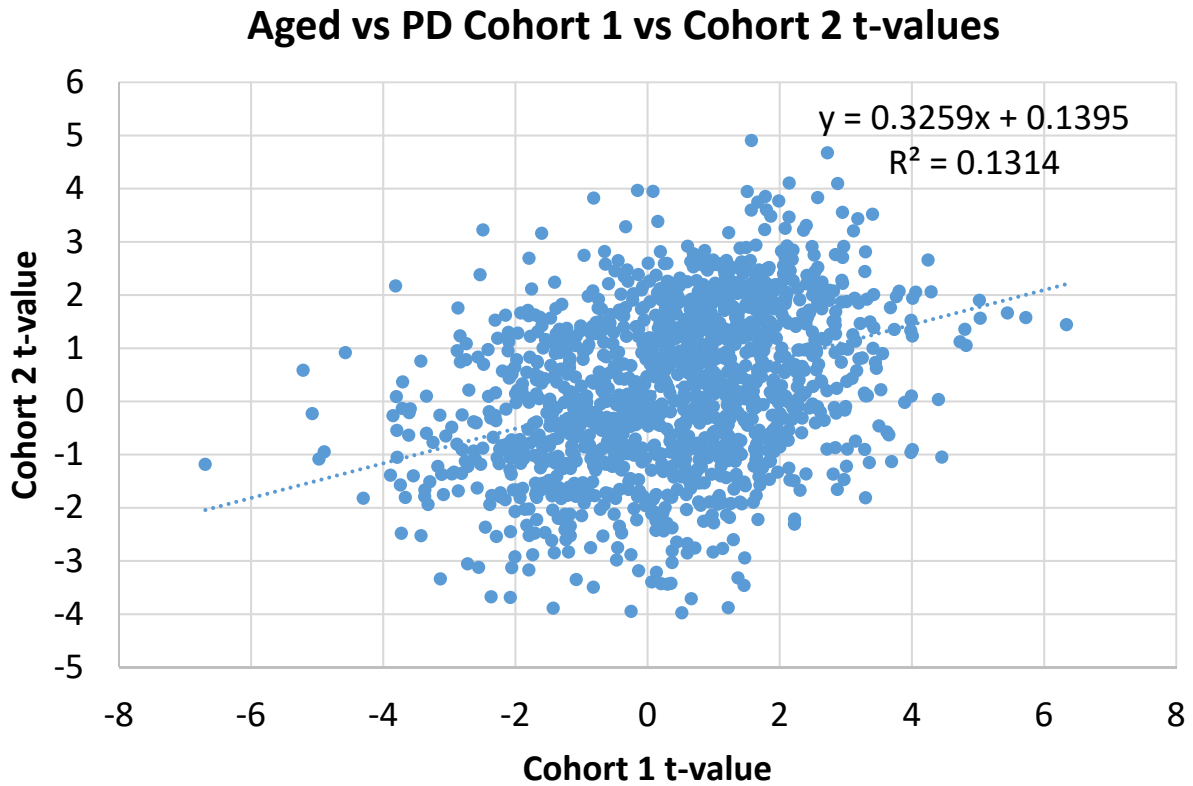


Supplementary Figure S 8. GSEA of differentially expressed human proteins young (<60 years) versus aged (>60 years). (B) Directed acyclic graph of GO terms.



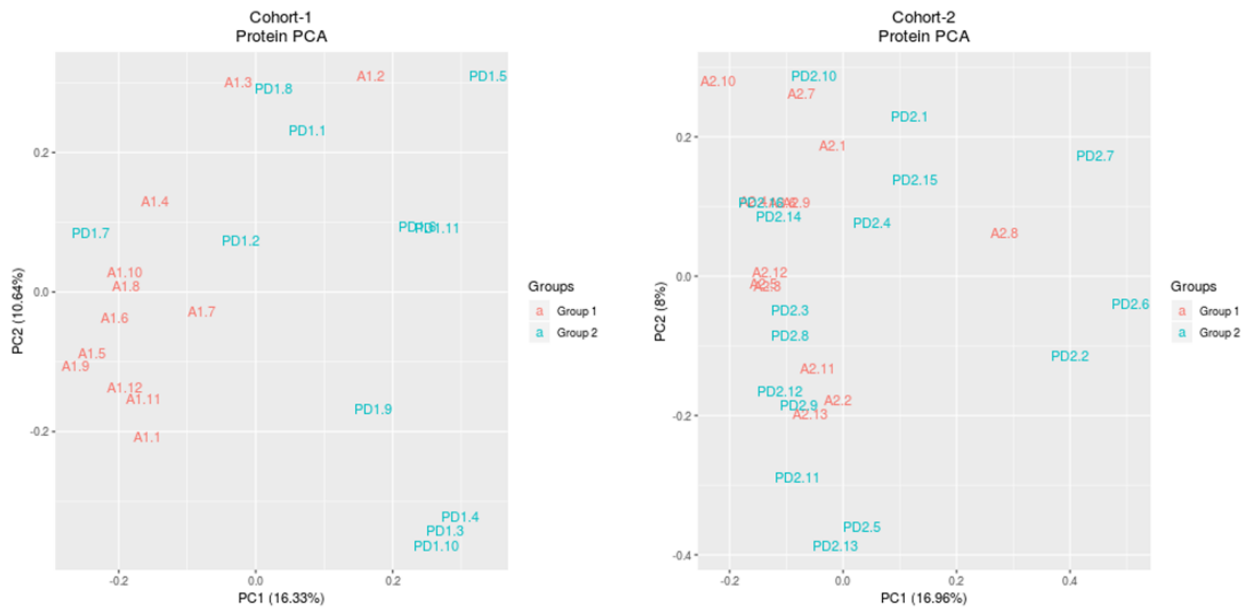
Supplementary Figure S 9. GSEA of differentially expressed human prefrontal cortex grey matter proteins observed in both cohort 1 and cohort, Aged (>60 years) versus PD,

(A) plot of differential abundance t-values for the two cohorts.



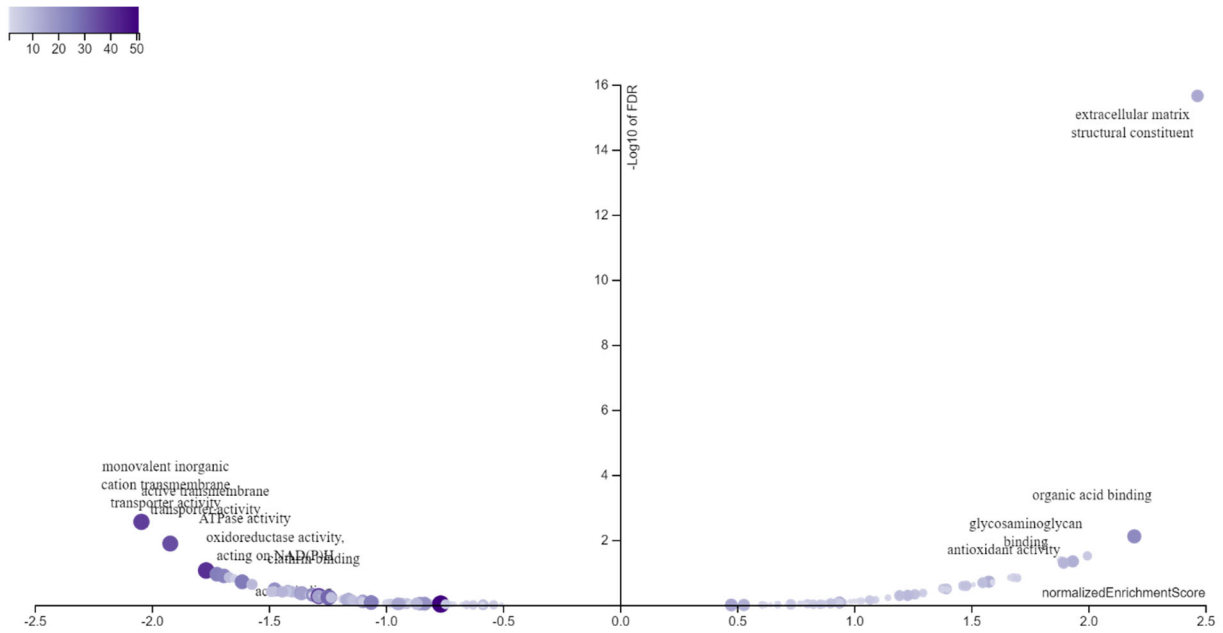
Supplementary Figure S 9. GSEA of differentially expressed human prefrontal cortex grey matter proteins observed in both cohort 1 and cohort 2, Aged (>60 years) versus PD,

(B) principal component analysis of cohort 1 and cohort 2



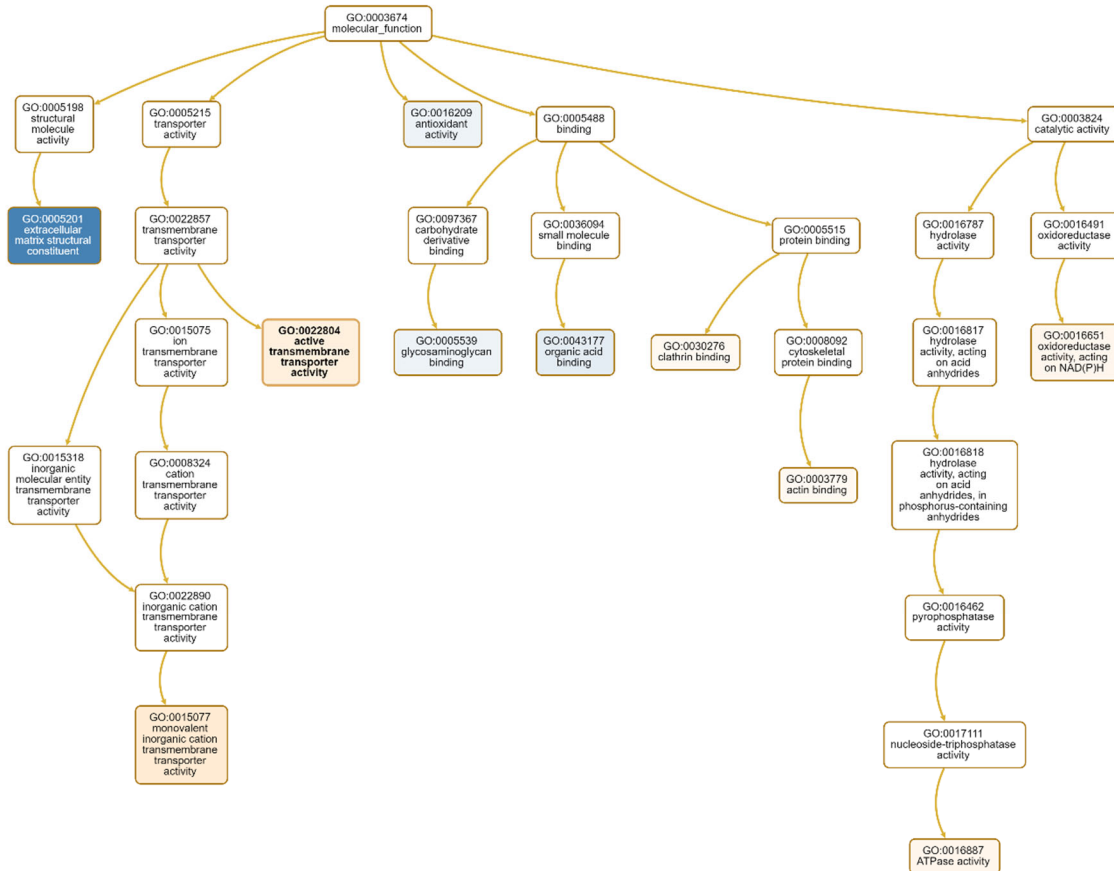
Supplementary Figure S 9. GSEA of differentially expressed human prefrontal cortex grey matter proteins observed in both cohort 1 and cohort 2, Aged (>60 years) versus PD.

(C) Volcano plot showing most enriched molecular functions

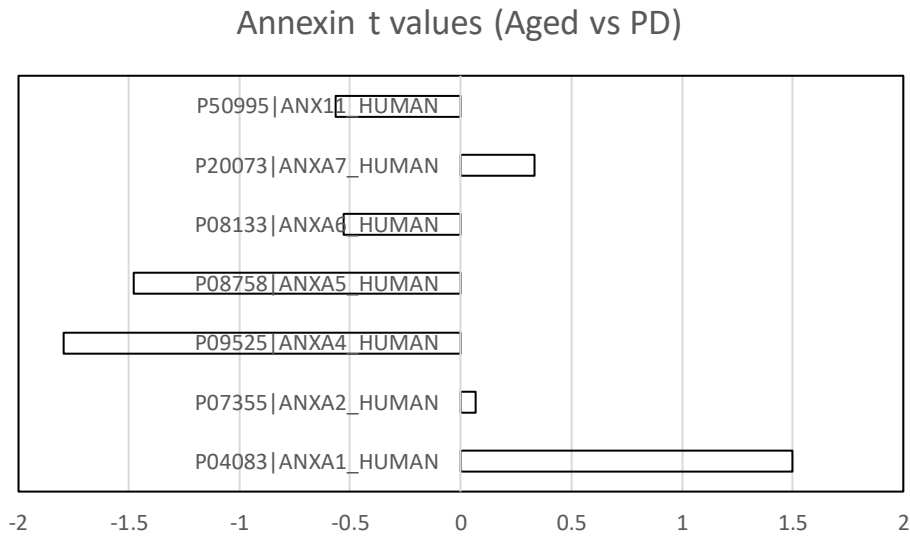


Supplementary Figure S 9. GSEA of differentially expressed human prefrontal cortex grey matter proteins observed in both cohort 1 and cohort 2, Aged (>60 years) versus PD.

(D) Directed acyclic graph of GO terms



Supplementary Figure S 10. Differential abundance t values for annexins in the human aged vs PD cohorts 1 and 2. Negative values are enriched in PD.



Supplementary Tables

Supplementary Table S 1A. Clinical data for control specimens.

| Cohort | Group | BU_ID | Death | SEX | Type of Brain | PMI | Cause of Death |
|--------|-------|--------|-------|------|---------------|-----|------------------------------------|
| 1 | Aged | C_0053 | 69 | Male | Control | 2 | Prostate Cancer |
| 1 | Aged | C_0002 | 73 | Male | Control | 2 | Acute myocardial infarction |
| 1 | Aged | C_0050 | 74 | Male | Control | 2 | Cardiac and/or respiratory failure |
| 1 | Aged | C_0060 | 76 | Male | Control | 2 | Pancreatic Cancer |
| 1 | Aged | C_0061 | 78 | Male | Control | 3 | Cardiac and/or respiratory failure |
| 1 | Aged | C_0009 | 81 | Male | Control | 3 | Cardiac and/or respiratory failure |
| 1 | Aged | C_0004 | 82 | Male | Control | 2 | Cardiorespiratory Arrest |
| 1 | Aged | C_0006 | 86 | Male | Control | 5 | Cardiac Arrest |
| 1 | Aged | C_0065 | 86 | Male | Control | 2 | CHF, Ischemic cardiomyopathy |
| 1 | Aged | C_0062 | 87 | Male | Control | 2 | Ruptured Aortic Aneurysm |
| 1 | Aged | C_0003 | 91 | Male | Control | 2 | Metastatic Bladder Cancer |
| 1 | Aged | C_0008 | 91 | Male | Control | 2 | End Stage Renal Disease |
| 2 | Young | C_0036 | 40 | Male | Control | 17 | Cardiac |
| 2 | Young | C_0033 | 43 | Male | Control | 15 | MI |
| 2 | Young | C_0037 | 44 | Male | Control | 28 | Cardiac Arrest |
| 2 | Young | C_0035 | 46 | Male | Control | 21 | Cardiac Arrest |
| 2 | Young | C_0075 | 52 | Male | control | 23 | Heart Attack |
| 2 | Young | C_0031 | 53 | Male | Control | 24 | MI |
| 2 | Young | C_0069 | 54 | Male | Control | 24 | Cardiac Arrest/CHF |
| 2 | Young | C_0081 | 55 | Male | Control | 26 | CPA-MI |
| 2 | Young | C_0082 | 57 | Male | Control | 18 | |
| 2 | Young | C_0038 | 57 | Male | Control | 20 | MI |
| 2 | Young | C_0077 | 36 | Male | control | 21 | electrocution |
| 2 | Young | C_0020 | 60 | Male | Control | 24 | MI |
| 2 | Aged | C_0087 | 64 | Male | Control | 19 | |
| 2 | Aged | C_0083 | 66 | Male | Control | 32 | CPN |
| 2 | Aged | C_0017 | 70 | Male | Control | 21 | MI |
| 2 | Aged | C_0039 | 80 | Male | Control | 15 | |
| 2 | Aged | C_0029 | 93 | Male | Control | 13 | Respiratory Failure; COPD |
| 2 | Aged | C_0005 | 97 | Male | Control | 2 | Metastatic Colon Cancer |
| 2 | Aged | C_0010 | 79 | Male | Control | 2 | Cardiac and/or respiratory failure |
| 2 | Aged | C_0013 | 69 | Male | Control | 15 | COPD |
| 2 | Aged | C_0024 | 69 | Male | Control | 26 | MI-CAD |
| 2 | Aged | C_0012 | 66 | Male | Control | 19 | MI |
| 2 | Aged | C_0018 | 66 | Male | Control | 17 | MI |
| 2 | Aged | C_0019 | 73 | Male | Control | 19 | COPD |
| 2 | Aged | C_0021 | 76 | Male | Control | 26 | Cardiac Arrest |

Supplementary Table S 1B. Clinical data for Parkinson's Disease specimens.

| Cohort | Group | BU_ID | Death | SEX | Motor Onset | Dementia | ALZ Pathology | PMI | Cause of Death |
|--------|-------|--------|-------|------|-------------|----------|---------------|-----|--|
| 1 | PD | P_0006 | 83 | Male | | 1 | absent | 2 | Pneumonia, hypertension, vascular dementia |
| 1 | PD | P_0012 | 80 | Male | 69 | 0 | absent | 2 | Probable MI |
| 1 | PD | P_0013 | 83 | Male | 79 | | absent | 2 | End Stage PD |
| 1 | PD | P_0014 | 80 | Male | 55 | | absent | 2 | End-Stage Parkinson's disease; inanition |
| 1 | PD | P_0015 | 84 | Male | 80 | 1 | absent | 2 | |
| 1 | PD | P_0016 | 88 | Male | 85 | 1 | absent | 2 | End-Stage COPD |
| 1 | PD | P_0018 | 81 | Male | 73 | 0 | absent | 2 | Small cell carcinoma of lung |
| 1 | PD | P_0019 | 77 | Male | 73 | 0 | absent | 4 | Cardiac and/or respiratory failure, severe MI |
| 1 | PD | P_0020 | 64 | Male | 59 | 0 | absent | 4 | Complications of lung cancer |
| 1 | PD | P_0021 | 85 | Male | | 1 | absent | 3 | Dementia; PD; DVD |
| 1 | PD | P_0034 | 64 | Male | 49 | 1 | absent | 4 | Failure to thrive secondary to PD, dementia, coronary artery disease |
| 1 | PD | P_0063 | 64 | Male | 53 | 0 | absent | 1 | |
| 2 | PD | P_0031 | 65 | Male | | | absent | 8 | |
| 2 | PD | P_0030 | 66 | Male | 55 | 0 | absent | 11 | PD |
| 2 | PD | P_0130 | 68 | Male | 62 | 1 | absent | 18 | MI |
| 2 | PD | P_0134 | 68 | Male | 63 | | mild | 23 | Cardiac Arrest |
| 2 | PD | P_0136 | 70 | Male | | | mild | 25 | |
| 2 | PD | P_0135 | 79 | Male | 66 | 0 | mild | 12 | Aspiration Pneumonia |
| 2 | PD | P_0023 | 80 | Male | 60 | 1 | absent | 27 | Pneumonia/PD |
| 2 | PD | P_0026 | 85 | Male | 65 | 0 | absent | 16 | PD |
| 2 | PD | P_0029 | 89 | Male | 72 | 0 | absent | 31 | End Stage Parkinson's Disease |
| 2 | PD | P_0022 | 94 | Male | | | absent | 9 | Respiratory Arrest/PD |
| 2 | PD | P_0132 | 95 | Male | 80 | 1 | absent | 16 | Parkinson's/Dementia |
| 2 | PD | P_0027 | 75 | Male | | | absent | 7 | Cardiac Arrest |
| 2 | PD | P_0028 | 74 | Male | | | absent | 15 | End Stage Parkinson's Disease; Bladder Infection |
| 2 | PD | P_0033 | 85 | Male | 71 | | absent | 19 | Cardiovascular Failure |
| 2 | PD | P_0126 | 75 | Male | 61 | 1 | mild | 30 | Aspiration Pneumonia |
| 2 | PD | P_0133 | 74 | Male | 66 | 0 | absent | 23 | Parkinson's disease |

Supplementary Table S 2A. Proteins from the organic acid binding gene set enriched in aged rat striatum from previously published data⁴.

| ID: GO:0043177; Name: organic acid binding | | | |
|---|---|-------------|--------|
| Size=27; leadingEdgeNum=11; enrichmentScore=0.61; normalizedEnrichmentScore=2.01; PValue=0.000e+0; FDR=9.763e-3 | | | |
| Gene Symbol | Gene Name | Entrez Gene | Score |
| Pgd | phosphogluconate dehydrogenase | 100360180 | 2.9471 |
| Vcan | versican | 114122 | 5.5605 |
| Ddc | dopa decarboxylase | 24311 | 2.3161 |
| Gad1 | glutamate decarboxylase 1 | 24379 | 2.3627 |
| Pc | pyruvate carboxylase | 25104 | 2.2401 |
| Bcan | brevican | 25393 | 1.9487 |
| Hapln1 | hyaluronan and proteoglycan link protein 1 | 29331 | 7.21 |
| C1qbp | complement C1q binding protein | 29681 | 5.0672 |
| Arhgdia | Rho GDP dissociation inhibitor alpha | 360678 | 1.9229 |
| Ddah1 | dimethylarginine dimethylaminohydrolase 1 | 64157 | 2.2448 |
| Rida | reactive intermediate imine deaminase A homolog | 65151 | 3.8715 |

Supplementary Table S 2B. Proteins from the structural constituent of ribosome gene set enriched in aged rat substantia nigra from previously published data⁴.

| ID: GO:0003735; Name: structural constituent of ribosome | | | |
|--|------------------------|-------------|---------|
| Size=23; leadingEdgeNum=13; enrichmentScore=-0.65; normalizedEnrichmentScore=-2.14; PValue=0.000e+0; FDR=1.216e-3 | | | |
| Gene Symbl | Gene Name | Entrez Gene | Score |
| Rps15a | ribosomal protein S15a | 117053 | -1.5369 |
| Rps16 | ribosomal protein S16 | 140655 | -2.7239 |
| Rpl15 | ribosomal protein L15 | 245981 | -1.6261 |
| Rpsa | ribosomal protein SA | 29236 | -1.913 |
| Rps14 | ribosomal protein S14 | 29284 | -3.3179 |
| Rps3a | ribosomal protein S3a | 29288 | -1.783 |
| Rps8 | ribosomal protein S8 | 65136 | -2.1854 |
| Rpl10a | ribosomal protein L10A | 81729 | -2.2221 |
| Rpl10 | ribosomal protein L10 | 81764 | -4.5484 |
| Rpl13 | ribosomal protein L13 | 81765 | -2.2695 |
| Rps24 | ribosomal protein S24 | 81776 | -2.7733 |
| Rps2 | ribosomal protein S2 | 83789 | -2.0951 |
| Rps27 | ribosomal protein S27 | 94266 | -1.5909 |

Supplementary Table S 3. Proteins from the human magnesium ion binding gene set enriched in aged human prefrontal cortex.

| ID: GO:0000287; Name: magnesium ion binding | | | |
|--|--|-------------|--------|
| Size=45; leadingEdgeNum=13; enrichmentScore=0.54; normalizedEnrichmentScore=1.97; PValue=0.000e+0; FDR=4.604e-2 | | | |
| Gene Symbol | Gene Name | Entrez Gene | Score |
| PDCD6 | programmed cell death 6 | 10016 | 2.4941 |
| FARSB | phenylalanyl-tRNA synthetase subunit beta | 10056 | 2.6126 |
| DUT | deoxyuridine triphosphatase | 1854 | 1.9156 |
| ENO1 | enolase 1 | 2023 | 4.1142 |
| ENO2 | enolase 2 | 2026 | 5.5922 |
| GNAI1 | G protein subunit alpha i1 | 2770 | 2.9079 |
| NME1 | NME/NM23 nucleoside diphosphate kinase 1 | 4830 | 1.4799 |
| PPA1 | pyrophosphatase (inorganic) 1 | 5464 | 2.691 |
| PRPSAP1 | phosphoribosyl pyrophosphate synthetase associated protein 1 | 5635 | 2.2597 |
| RAN | RAN, member RAS oncogene family | 5901 | 7.7422 |
| RAP2A | RAP2A, member of RAS oncogene family | 5911 | 2.0748 |
| RHEB | Ras homolog, mTORC1 binding | 6009 | 1.6632 |
| SNCA | synuclein alpha | 6622 | 2.2621 |

Supplementary Table S 4A. Proteins from the extracellular matrix structural component gene set enriched in human prefrontal cortex comparing unaffected aged versus PD specimens.

| ID: GO:0005201; Name: extracellular matrix structural constituent | | | | |
|---|-------------|---|-------------|--------|
| Size=21; leadingEdgeNum=14; enrichmentScore=0.69; normalizedEnrichmentScore=2.47; PValue=0.000e+0; FDR=0.000e+0 | | | | |
| User ID | Gene Symbol | Gene Name | Entrez Gene | Score |
| 1277 | COL1A1 | collagen type I alpha 1 chain | 1277 | 2.7486 |
| 1278 | COL1A2 | collagen type I alpha 2 chain | 1278 | 2.4472 |
| 1280 | COL2A1 | collagen type II alpha 1 chain | 1280 | 2.4159 |
| 1281 | COL3A1 | collagen type III alpha 1 chain | 1281 | 1.7167 |
| 1282 | COL4A1 | collagen type IV alpha 1 chain | 1282 | 1.7107 |
| 1284 | COL4A2 | collagen type IV alpha 2 chain | 1284 | 1.384 |
| 1293 | COL6A3 | collagen type VI alpha 3 chain | 1293 | 1.9479 |
| 1404 | HAPLN1 | hyaluronan and proteoglycan link protein 1 | 1404 | 1.0703 |
| 1462 | VCAN | versican | 1462 | 1.9737 |
| 2243 | FGA | fibrinogen alpha chain | 2243 | 0.9566 |
| 2244 | FGB | fibrinogen beta chain | 2244 | 0.948 |
| 2266 | FGG | fibrinogen gamma chain | 2266 | 1.1769 |
| 3371 | TNC | tenascin C | 3371 | 2.3006 |
| 64129 | TINAGL1 | tubulointerstitial nephritis antigen like 1 | 64129 | 1.2354 |

Supplementary Table S 4B. Proteins from the organic acid binding gene set enriched in human prefrontal cortex comparing unaffected aged versus PD specimens.

| User ID | Gene Symbol | Gene Name | Entrez Gene | Score |
|---|-------------|--|-------------|--------|
| ID: GO:0043177; Name: organic acid binding | | | | |
| Size=40; leadingEdgeNum=22; enrichmentScore=0.51; normalizedEnrichmentScore=2.20; PValue=0.000e+0; FDR=7.733e-3 | | | | |
| 10247 | RIDA | reactive intermediate imine deaminase A homolog | 10247 | 1.4752 |
| 128 | ADH5 | alcohol dehydrogenase 5 (class III), chi polypeptide | 128 | 1.9285 |
| 1404 | HAPLN1 | hyaluronan and proteoglycan link protein 1 | 1404 | 1.0703 |
| 1462 | VCAN | versican | 1462 | 1.9737 |
| 1463 | NCAN | neurocan | 1463 | 0.9841 |
| 2171 | FABP5 | fatty acid binding protein 5 | 2171 | 0.922 |
| 23564 | DDAH2 | dimethylarginine dimethylaminohydrolase 2 | 23564 | 0.888 |
| 2571 | GAD1 | glutamate decarboxylase 1 | 2571 | 1.999 |
| 3039 | HBA1 | hemoglobin subunit alpha 1 | 3039 | 1.9761 |
| 3043 | HBB | hemoglobin subunit beta | 3043 | 2.6973 |
| 3047 | HBG1 | hemoglobin subunit gamma 1 | 3047 | 1.2441 |
| 3048 | HBG2 | hemoglobin subunit gamma 2 | 3048 | 1.2441 |
| 4099 | MAG | myelin associated glycoprotein | 4099 | 1.1416 |
| 445 | ASS1 | argininosuccinate synthase 1 | 445 | 2.4563 |
| 5660 | PSAP | prosaposin | 5660 | 2.0956 |
| 5730 | PTGDS | prostaglandin D2 synthase | 5730 | 1.397 |
| 5836 | PYGL | glycogen phosphorylase L | 5836 | 0.8199 |
| 5917 | RARS | arginyl-tRNA synthetase | 5917 | 1.7961 |
| 60484 | HAPLN2 | hyaluronan and proteoglycan link protein 2 | 60484 | 1.2884 |
| 6262 | RYR2 | ryanodine receptor 2 | 6262 | 1.5447 |
| 63827 | BCAN | brevican | 63827 | 1.1992 |
| 9380 | GRHPR | glyoxylate and hydroxypyruvate reductase | 9380 | 1.8283 |

Supplementary Table S 5. Proteins from the glycosaminoglycan binding gene set enriched in prefrontal cortex comparing unaffected aged versus PD specimens.

| ID: GO:0005539; Name: glycosaminoglycan binding | | | | |
|---|-------------|--|-------------|--------|
| Size=19; leadingEdgeNum=13; enrichmentScore=0.55; normalizedEnrichmentScore=1.93; PValue=0.000e+0; FDR=4.551e-2 | | | | |
| User ID | Gene Symbol | Gene Name | Entrez Gene | Score |
| 1404 | HAPLN1 | hyaluronan and proteoglycan link protein 1 | 1404 | 1.0703 |
| 1462 | VCAN | versican | 1462 | 1.9737 |
| 1463 | NCAN | neurocan | 1463 | 0.9841 |
| 1809 | DPYSL3 | dihydropyrimidinase like 3 | 1809 | 0.5917 |
| 307 | ANXA4 | annexin A4 | 307 | 1.7921 |
| 308 | ANXA5 | annexin A5 | 308 | 1.4768 |
| 309 | ANXA6 | annexin A6 | 309 | 0.5305 |
| 351 | APP | amyloid beta precursor protein | 351 | 1.5335 |
| 5048 | PAFAH1B1 | platelet activating factor acetylhydrolase 1b regulatory subunit 1 | 5048 | 1.3738 |
| 5621 | PRNP | prion protein | 5621 | 0.7385 |
| 5802 | PTPRS | protein tyrosine phosphatase, receptor type S | 5802 | 0.5632 |
| 60484 | HAPLN2 | hyaluronan and proteoglycan link protein 2 | 60484 | 1.2884 |
| 63827 | BCAN | brevican | 63827 | 1.1992 |

Supplementary Table S 6. Proteins from the monovalent inorganic cation transmembrane transporter activity gene set enriched in prefrontal cortex comparing unaffected aged versus PD specimens.

| ID: GO:0015077; Name: monovalent inorganic cation transmembrane transporter activity | | | | |
|--|-------------|---|-------------|---------|
| Size=58; leadingEdgeNum=38; enrichmentScore=-0.56; normalizedEnrichmentScore=-2.04; PValue=0.000e+0; | | | | |
| FDR=2.768e-3 | | | | |
| User ID | Gene Symbol | Gene Name | Entrez Gene | Score |
| 10476 | ATP5PD | ATP synthase peripheral stalk subunit d | 10476 | -1.8608 |
| 1327 | COX4I1 | cytochrome c oxidase subunit 4I1 | 1327 | -2.541 |
| 1337 | COX6A1 | cytochrome c oxidase subunit 6A1 | 1337 | -2.8616 |
| 1345 | COX6C | cytochrome c oxidase subunit 6C | 1345 | -1.7636 |
| 23530 | NNT | nicotinamide nucleotide transhydrogenase | 23530 | -1.2948 |
| 388662 | SLC6A17 | solute carrier family 6 member 17 | 388662 | -1.7863 |
| 3954 | LETM1 | leucine zipper and EF-hand containing transmembrane protein 1 | 3954 | -1.4236 |
| 4697 | NDUFA4 | NDUFA4, mitochondrial complex associated | 4697 | -1.155 |
| 478 | ATP1A3 | ATPase Na ⁺ /K ⁺ transporting subunit alpha 3 | 478 | -1.6018 |
| 479 | ATP12A | ATPase H ⁺ /K ⁺ transporting non-gastric alpha2 subunit | 479 | -1.238 |
| 482 | ATP1B2 | ATPase Na ⁺ /K ⁺ transporting subunit beta 2 | 482 | -1.1537 |
| 488 | ATP2A2 | ATPase sarcoplasmic/endoplasmic reticulum Ca ²⁺ transporting 2 | 488 | -2.7324 |
| 506 | ATP5F1B | ATP synthase F1 subunit beta | 506 | -1.941 |
| 509 | ATP5F1C | ATP synthase F1 subunit gamma | 509 | -2.1328 |
| 51382 | ATP6V1D | ATPase H ⁺ transporting V1 subunit D | 51382 | -1.0793 |
| 515 | ATP5PB | ATP synthase peripheral stalk-membrane subunit b | 515 | -1.54 |
| 51606 | ATP6V1H | ATPase H ⁺ transporting V1 subunit H | 51606 | -1.4659 |
| 523 | ATP6V1A | ATPase H ⁺ transporting V1 subunit A | 523 | -3.1106 |
| 5250 | SLC25A3 | solute carrier family 25 member 3 | 5250 | -2.0836 |
| 526 | ATP6V1B2 | ATPase H ⁺ transporting V1 subunit B2 | 526 | -1.1876 |
| 528 | ATP6V1C1 | ATPase H ⁺ transporting V1 subunit C1 | 528 | -1.5198 |
| 529 | ATP6V1E1 | ATPase H ⁺ transporting V1 subunit E1 | 529 | -2.0498 |
| 535 | ATP6V0A1 | ATPase H ⁺ transporting V0 subunit a1 | 535 | -1.5103 |
| 537 | ATP6AP1 | ATPase H ⁺ transporting accessory protein 1 | 537 | -1.8737 |
| 539 | ATP5PO | ATP synthase peripheral stalk subunit OSCP | 539 | -1.969 |
| 57030 | SLC17A7 | solute carrier family 17 member 7 | 57030 | -1.641 |
| 57282 | SLC4A10 | solute carrier family 4 member 10 | 57282 | -2.8476 |
| 57468 | SLC12A5 | solute carrier family 12 member 5 | 57468 | -1.0233 |
| 6506 | SLC1A2 | solute carrier family 1 member 2 | 6506 | -2.3548 |
| 6507 | SLC1A3 | solute carrier family 1 member 3 | 6507 | -1.887 |
| 6543 | SLC8A2 | solute carrier family 8 member A2 | 6543 | -1.4728 |
| 6616 | SNAP25 | synaptosome associated protein 25 | 6616 | -3.5623 |
| 79751 | SLC25A22 | solute carrier family 25 member 22 | 79751 | -1.6384 |
| 8514 | KCNAB2 | potassium voltage-gated channel subfamily A regulatory beta subu | 8514 | -1.3135 |
| 8671 | SLC4A4 | solute carrier family 4 member 4 | 8671 | -2.3251 |
| 9114 | ATP6V0D1 | ATPase H ⁺ transporting V0 subunit d1 | 9114 | -1.7036 |
| 9296 | ATP6V1F | ATPase H ⁺ transporting V1 subunit F | 9296 | -1.2432 |
| 9377 | COX5A | cytochrome c oxidase subunit 5A | 9377 | -0.9858 |

Supplementary Table S 7. Proteins from the active transmembrane transporter activity gene set negatively enriched in prefrontal cortex comparing unaffected aged versus PD specimens.

| ID: GO:0022804; Name: active transmembrane transporter activity | | | | |
|--|----------|---|--------|---------|
| Size=54; leadingEdgeNum=35; enrichmentScore=-0.53; normalizedEnrichmentScore=-1.92; PValue=0.000e+0; | | | | |
| FDR=1.292e-2 | | | | |
| 10476 | ATP5PD | ATP synthase peripheral stalk subunit d | 10476 | -1.8608 |
| 292 | SLC25A5 | solute carrier family 25 member 5 | 292 | -1.4848 |
| 388662 | SLC6A17 | solute carrier family 6 member 17 | 388662 | -1.7863 |
| 3954 | LETM1 | leucine zipper and EF-hand containing transmembrane protein 1 | 3954 | -1.4236 |
| 478 | ATP1A3 | ATPase Na ⁺ /K ⁺ transporting subunit alpha 3 | 478 | -1.6018 |
| 479 | ATP12A | ATPase H ⁺ /K ⁺ transporting non-gastric alpha2 subunit | 479 | -1.238 |
| 482 | ATP1B2 | ATPase Na ⁺ /K ⁺ transporting subunit beta 2 | 482 | -1.1537 |
| 488 | ATP2A2 | ATPase sarcoplasmic/endoplasmic reticulum Ca ²⁺ transporting 2 | 488 | -2.7324 |
| 490 | ATP2B1 | ATPase plasma membrane Ca ²⁺ transporting 1 | 490 | -1.4004 |
| 491 | ATP2B2 | ATPase plasma membrane Ca ²⁺ transporting 2 | 491 | -1.4387 |
| 492 | ATP2B3 | ATPase plasma membrane Ca ²⁺ transporting 3 | 492 | -2.0022 |
| 493 | ATP2B4 | ATPase plasma membrane Ca ²⁺ transporting 4 | 493 | -2.1314 |
| 506 | ATP5F1B | ATP synthase F1 subunit beta | 506 | -1.941 |
| 509 | ATP5F1C | ATP synthase F1 subunit gamma | 509 | -2.1328 |
| 51382 | ATP6V1D | ATPase H ⁺ transporting V1 subunit D | 51382 | -1.0793 |
| 515 | ATP5PB | ATP synthase peripheral stalk-membrane subunit b | 515 | -1.54 |
| 51606 | ATP6V1H | ATPase H ⁺ transporting V1 subunit H | 51606 | -1.4659 |
| 523 | ATP6V1A | ATPase H ⁺ transporting V1 subunit A | 523 | -3.1106 |
| 5250 | SLC25A3 | solute carrier family 25 member 3 | 5250 | -2.0836 |
| 526 | ATP6V1B2 | ATPase H ⁺ transporting V1 subunit B2 | 526 | -1.1876 |
| 528 | ATP6V1C1 | ATPase H ⁺ transporting V1 subunit C1 | 528 | -1.5198 |
| 529 | ATP6V1E1 | ATPase H ⁺ transporting V1 subunit E1 | 529 | -2.0498 |
| 535 | ATP6V0A1 | ATPase H ⁺ transporting V0 subunit a1 | 535 | -1.5103 |
| 537 | ATP6AP1 | ATPase H ⁺ transporting accessory protein 1 | 537 | -1.8737 |
| 539 | ATP5PO | ATP synthase peripheral stalk subunit OSCP | 539 | -1.969 |
| 57030 | SLC17A7 | solute carrier family 17 member 7 | 57030 | -1.641 |
| 57282 | SLC4A10 | solute carrier family 4 member 10 | 57282 | -2.8476 |
| 6506 | SLC1A2 | solute carrier family 1 member 2 | 6506 | -2.3548 |
| 6507 | SLC1A3 | solute carrier family 1 member 3 | 6507 | -1.887 |
| 6509 | SLC1A4 | solute carrier family 1 member 4 | 6509 | -3.0523 |
| 6543 | SLC8A2 | solute carrier family 8 member A2 | 6543 | -1.4728 |
| 79751 | SLC25A22 | solute carrier family 25 member 22 | 79751 | -1.6384 |
| 8671 | SLC4A4 | solute carrier family 4 member 4 | 8671 | -2.3251 |
| 9114 | ATP6V0D1 | ATPase H ⁺ transporting V0 subunit d1 | 9114 | -1.7036 |
| 9296 | ATP6V1F | ATPase H ⁺ transporting V1 subunit F | 9296 | -1.2432 |

Supplementary References

- 1 Raghunathan, R., Sethi, M. & Zaia, J. On-slide tissue digestion for mass spectrometry based glycomic and proteomic profiling. *MethodsX* **6**, 2329-2347, doi:<https://doi.org/10.1016/j.mex.2019.09.029> (2019).
- 2 Esko, J. D. & Selleck, S. B. Order out of chaos: assembly of ligand binding sites in heparan sulfate. *Annu Rev Biochem* **71**, 435-471 (2002).
- 3 Lindahl, U. & Li, J. P. Interactions between heparan sulfate and proteins-design and functional implications. *Int Rev Cell Mol Biol* **276**, 105-159, doi:10.1016/S1937-6448(09)76003-4 (2009).
- 4 Raghunathan, R. *et al.* Glycomic and Proteomic Changes in Aging Brain Nigrostriatal Pathway. *Molecular & Cellular Proteomics* **17**, 1778-1787, doi:10.1074/mcp.RA118.000680 (2018).